57-second oscillations in Nova Centauri 1986 (V842 Cen)

Patrick A. Woudt,[1]* Brian Warner,[1] Julian Osborne[2] and Kim Page[2]

[1]*Department of Astronomy, University of Cape Town, Private Bag X3, Rondebosch 7701, South Africa*
[2]*Department of Physics and Astronomy, University of Leicester, University Road, Leicester LE1 7RH*

ABSTRACT

High-speed photometry in 2008 shows that the light curve of V842 Cen possesses a coherent modulation at 56.825 s, with sidebands at 56.598 and 57.054 s. These have appeared since this nova remnant was observed in 2000 and 2002. We deduce that the dominant signal is the rotation period of the white dwarf primary and the sidebands are caused by reprocessing from a surface moving with an orbital period of 3.94 h. Thus, V842 Cen is an intermediate polar (IP) of the DQ Herculis subclass, is the fastest rotating white dwarf among the IPs and is the third fastest known in a cataclysmic variable. As in other IPs, we see no dwarf nova oscillations, but there are often quasi-periodic oscillations in the range 350–1500 s. There is a strong brightness modulation with a period of 3.78 h, which we attribute to negative superhumps, and there is an even stronger signal at 2.886 h which is of unknown origin but is probably a further example of that seen in GW Lib and some other systems. We used the *Swift* satellite to observe V842 Cen in the ultraviolet and in X-rays, although no periodic modulation was detected in the short observations. The X-ray luminosity of this object appears to be much lower than that of other IPs in which the accretion region is directly visible.

Key words: binaries: close – stars: individual: V842 Cen – novae, cataclysmic variables – stars: oscillations.

1 INTRODUCTION

Nova Centauri 1986 (later designated V842 Cen) was discovered on 1986 November 22 at $V = 5.6$ and two days later reached maximum at $V = 4.6$ (McNaught 1986). It was a moderately fast nova, with decay time $t_3 = 48$ d and developed an obscuring dust shell starting 37 d after maximum and reaching greatest optical thickness 74 d after maximum, placing it in the group II category of nova light curves as defined by Duerbeck (1981), which is essentially of DQ Herculis type. The pre-eruption brightness was estimated by McNaught (1986) to be in the range $B \sim 18.0$–18.6. Fifteen years after eruption, it was at $V \sim 15.8$ (Downes & Duerbeck 2000; Woudt & Warner 2003, hereafter WW03), and our latest measurements give $V \sim 16.3$. Therefore, 22 years after maximum it is still about two magnitudes above its pre-nova brightness, which could be a result of irradiation enhanced mass transfer caused by a still very hot white dwarf primary, especially if it is relatively massive [see Warner (2002) for a discussion of anomalous post-nova luminosities arising from this effect], though Kato (private communication) reports that there is nothing in the eruptive behaviour to suggest a mass much greater than $0.7\,M_\odot$. DQ Her, also a moderately fast nova ($t_3 = 94$ d), but of low mass ($0.60\,M_\odot$; Horne, Welsh & Wade 1993), reached its maximum optical thickness dust obscured phase

101 d after maximum light; it was at $m_{pg} \sim 14.8$ prior to its 1934 eruption (Robinson 1975) and yet had returned to that level less than 20 yr later (Walker 1956).

Sekiguchi et al. (1989) give distance estimates that average 1.0 kpc from strengths of interstellar Na D lines and the 2200 Å feature, and a reddening of $E(B - V) = 0.55$. Gill & O'Brien (1998) in 1995 detected an ejecta shell of diameter $\sim$1.5 arcsec in direct imaging.

There is nothing in the nova development of V842 Cen that marks it as in any way peculiar. The ultraviolet (UV) and soft X-ray turn-off times are normal (González-Riestra, Orio & Gallagher 1998) and the abundances (including a high carbon content typical of dusty ejecta) are within the normal ranges (Andrea, Drechsel & Starrfield 1994), except that Iben (1992) found that V842 Cen was the only nova with a He/H ratio falling between two groups having solar and half-solar values.

Recent spectra, however, show peculiarities that are relevant to the present state of the primary in V842 Cen. An optical spectrum obtained in 2003 (Schmidtobreick et al. 2005) shows a strong blue continuum with weak high ionization lines, e.g. C IV, probably coming from the nova ejecta but indicative of a hot central source, yet accompanied by strong Balmer lines extending to high-series components and by He I emission lines, with only moderate He II and 4650 Å Bowen fluorescence lines. These are more characteristic of dwarf novae spectra than of old novae. Schmidtobreick et al. (2005) find that the much older nova XX Tau (Nova Tauri 1927, $t_3 = 42$ d)

*E-mail: Patrick.Woudt@uct.ac.za

has a similar unusual emission line spectrum and suggest that both of these novae could be currently in states of low rates of mass transfer ($\dot{M}$).

Finally, previous high-speed photometry of V842 Cen, carried out in 2000 (WW03), showed extreme activity with flares up to 0.25 mag on time-scales ∼5 min but no evident orbital or short-period coherent brightness modulations, though there were quasi-periodic oscillations (QPOs) on time-scales ∼1000 s. A parallel was drawn with the light curve of TT Ari, which is a high $\dot{M}$ nova-like cataclysmic variable (CV).

With a view to checking whether V842 Cen had changed its light-curve character in the 8 years since it was last observed, we made an initial exploration in 2008 February, and the surprising result led us to concentrate on it for the remainder of that and the following observing run. The optical observations are described and analysed in Section 2, X-ray observations in Section 3 and a discussion is given in Section 4.

2 OPTICAL OBSERVATIONS AND ANALYSIS

Our observations were made with the University of Cape Town's frame transfer CCD photometer (O'Donoghue 1995) attached to the 74-in Radcliffe telescope at the Sutherland site of the South African Astronomical Observatory. All photometry was unfiltered (i.e. in white light), with 6-s integrations, and a white dwarf standard star was used to provide an approximate V magnitude scale. The observing runs are listed in Table 1.

Fig. 1 shows the light curves for 2008 February (note that V842 Cen was only accessible at the end of the night for a maximum of about 4 h) and Fig. 2 shows the 2008 March light curves. In the latter, we have phased the light curves on a period of 3.780 h, for reasons explained below.
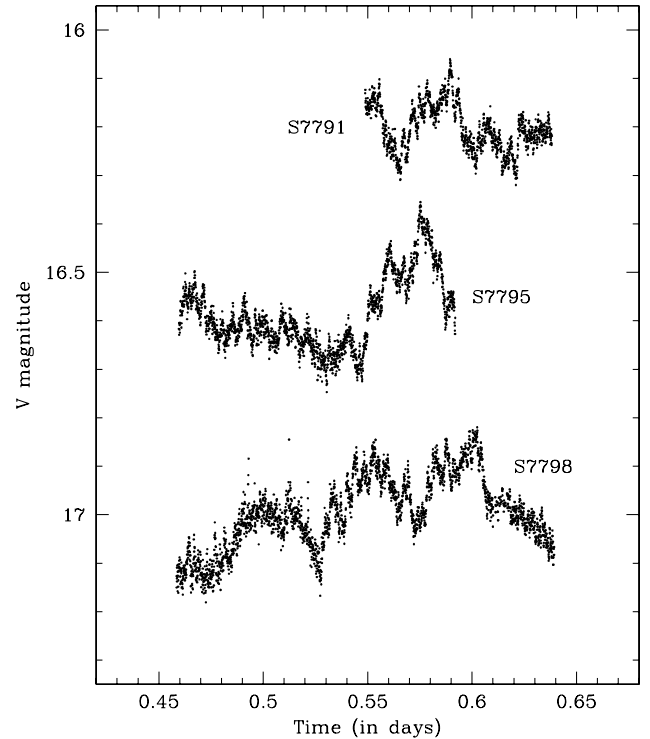
Comparison with the 2000 light curves (WW03) shows one immediately obvious change – there are now recurrent peaks of amplitude ∼0.3 mag on a time-scale ∼4 h. A more subtle addition appears when comparing the high-frequency parts of the Fourier transforms (FTs) of individual runs in 2000 June, 2008 February and 2008 March. As seen in Fig. 3, a modulation at ∼57 s has appeared in the interval. There is no sign of this in a short run made in 2002 March (WW03).
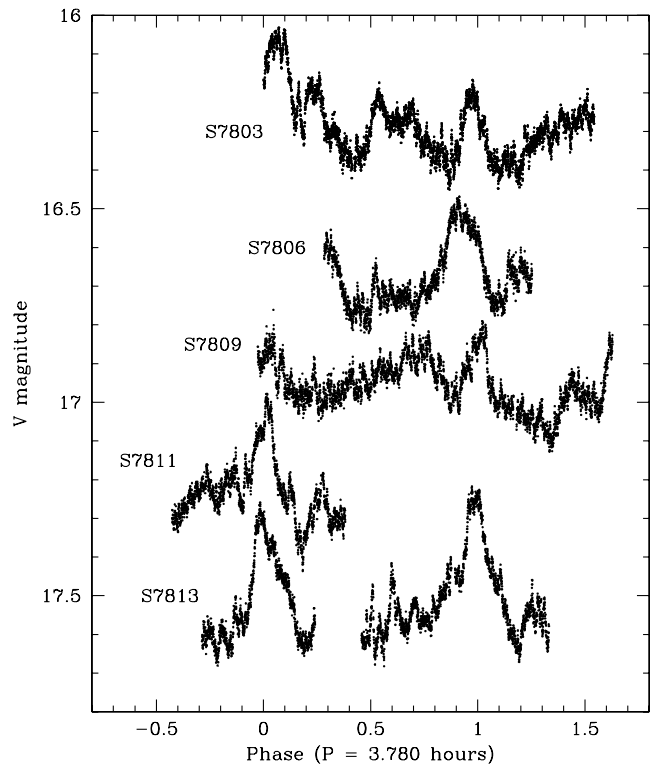
2.1 The 57-s brightness oscillation

We start our analysis by concentrating on the neighbourhood of the ∼57 s signal. The FT for the combined 2008 March light curves, which have a 5-d baseline, is shown in Fig. 4(a) (we have omitted run S7813 where the interruption in the light curve causes problems in the FT). The dominant feature is the window pattern of the data

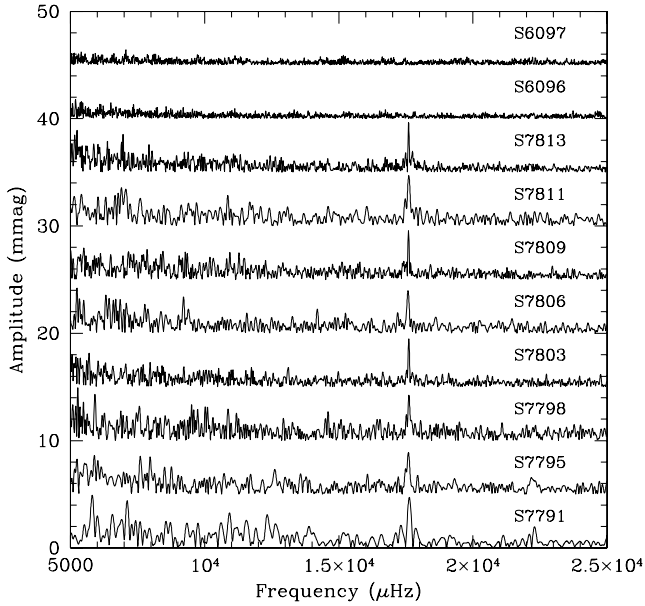**Table 1.** Observing log of photometric observations.

Run	Date of obs. (start of night)	HJD of first obs. (+245 0000.0)	Length (h)	V (mag)
S7791	2008 February 17	4514.54882	2.14	16.2
S7795	2008 February 18	4515.45960	3.18	16.3
S7798	2008 February 19	4516.45845	4.34	16.3
S7803	2008 March 13	4539.41017	5.83	16.3
S7806	2008 March 14	4540.39963	3.67	16.3
S7809	2008 March 16	4542.39838	6.25	16.3
S7811	2008 March 17	4543.43785	3.05	16.3
S7813	2008 March 18	4544.40490	6.12	16.2

Figure 1. The light curves of V842 Cen obtained in 2008 February. The light curves of S7795 and S7798 have been displaced vertically for display purposes by 0.3 and 0.7 mag, respectively.

Figure 2. The light curves of V842 Cen obtained in 2008 March. The light curves of S7806, S7809, S7811 and S7811 have been displaced vertically for display purposes only.
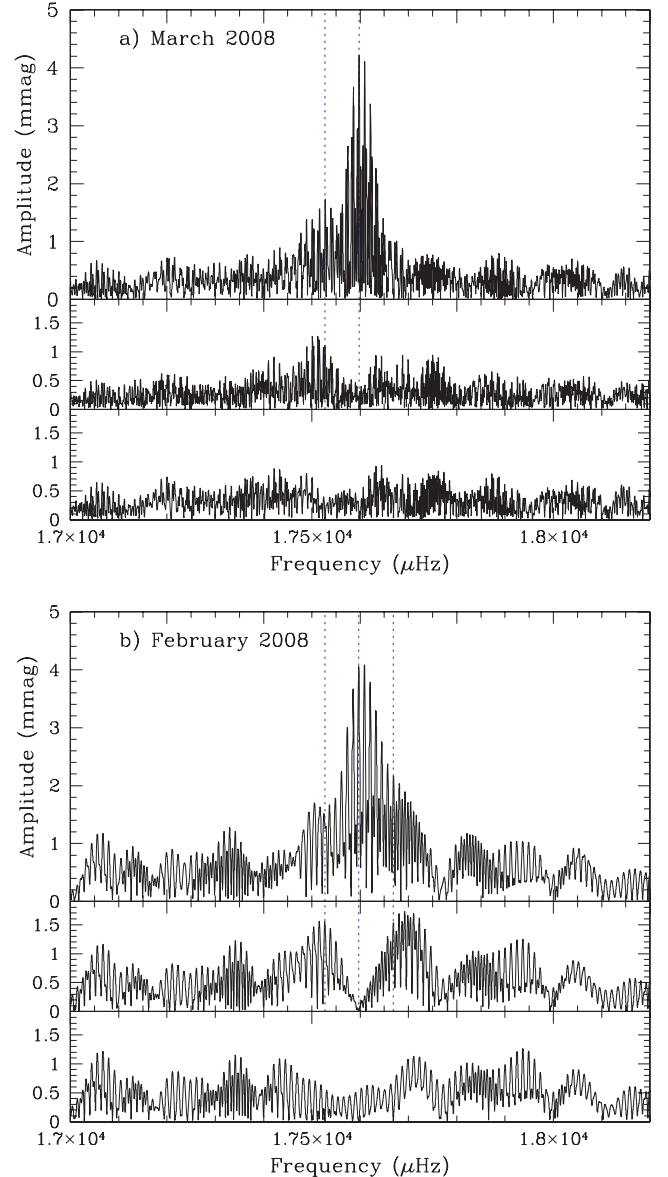
Figure 3. High-frequency FTs of the individual observing runs of V842 Cen.

set, centred on 56.825 ± 0.001 s, with an amplitude of 4.2 mmag (we estimate uncertainties from the formal errors of fitting sine curves by least squares). Prewhitening with that modulation leaves a signal on the low-frequency side [visible at the position of the dashed line in Fig. 4(a)] with period 57.054 ± 0.002 s and amplitude 1.6 mmag. This is equivalent to a sideband splitting of 70.5 ± 0.5 μHz. Prewhitening with both sinusoids simultaneously leaves no significant signal in this region, as seen in the lower plot in Fig. 4(a).
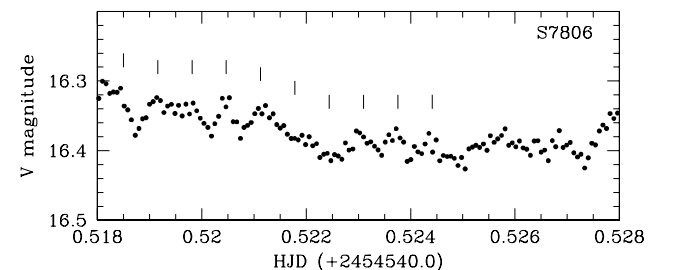
The FT for the combined 2008 February light curves is shown in Fig. 4(b). The dominant signal over the 3-d baseline is at 56.828 ± 0.002 s, and amplitude of 3.9 mmag. The periods and amplitudes in the two data sets indicate a stable modulation, within errors of measurement. As can be seen in the FT, the lower frequency sideband is also present, but there is evidence for a longer frequency sideband overlapping the principal window pattern. A three sinusoid fit to the light curve gives 57.055 and 56.598 s for the two sidebands, both with uncertainty ±0.005 s and amplitude 1.7 mmag. Prewhitening with these three modulations leaves no significant signal in the region, as seen in the lower plot of Fig. 4(b).

The frequency difference between the principal signal and the longer frequency sideband is 71.6 ± 2.3 μHz, which is within errors the same as the splitting on the low-frequency side. This arrangement, of equally split sidebands, even with a variation of amplitude in one sideband, is the recognizable structure of an intermediate polar (IP). Denoting the spin frequency of the white dwarf primary as ω and the orbital frequency as Ω, we have detected the components $\omega, \omega - \Omega$ and $\omega + \Omega$, which are characteristic of an IP (Warner 1986). The variable amplitude of the one sideband is consistent with reprocessed radiation from a rotating source, not simply amplitude modulation of a single source.

The FTs for individual runs do not resolve the sidebands and as a result the amplitude of the 57-s modulation varies on the 70.0 μHz, or 3.94 h, time-scale. Selecting a section where the amplitude is maximal enables us to show the 57 s directly in the light curve (Fig. 5).

Figure 4. FTs in the vicinity of the 57-s oscillations: (a) 2008 March (top diagram), (b) 2008 February (bottom diagram). The 57-s oscillation and its orbital sidebands are marked by the dashed vertical lines. The middle and lower panels in both diagrams show the FTs after prewhitening with the 57-s oscillation only (middle panels), and the 57-s oscillations plus the identified orbital sidebands simultaneously (lower panels), respectively.
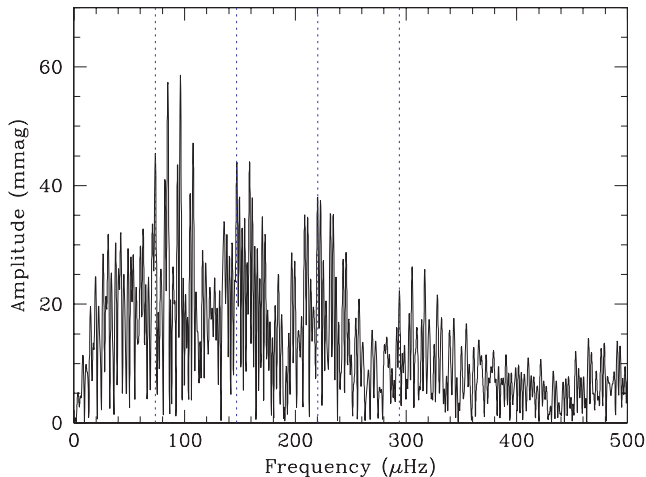

Figure 5. A section of the light curve of run S7806. The 57-s oscillations are marked by the vertical bars.
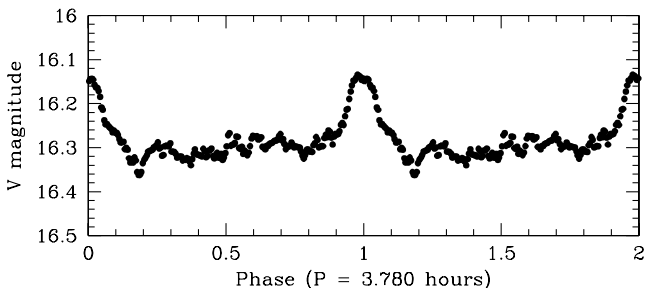
In the FTs, there are no signs of harmonics or a subharmonic to the 57-s modulations. The uncertainties in the 56.825 s signal are just too large to enable the gap between the 2008 February and March observations to be bridged without ambiguity, so a more accurate period cannot be offered.
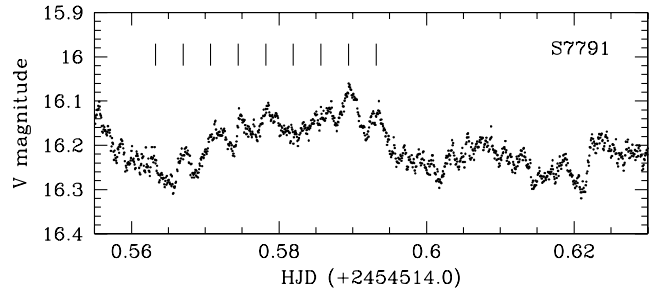
2.2 Orbital and superhump periods

We now turn to the low-frequency end of the FTs, seen in Fig. 6 for the 2008 March runs (the February data are too sparse to give useful additional information). The strongest signal is at 96.23 ± 0.01 μHz, or 2.886 h, with amplitude 60 mmag and no detectable harmonics, which we will discuss later. Prewhitening at that frequency leaves a strong signal at 73.46 ± 0.07 μHz, or 3.780 h and strong higher harmonics. This is the period chosen to phase the light curves in Fig. 2. The average light curve of the 2008 March data at this period is shown in Fig. 7. From the general appearance of the light curve – its narrow and variable peak profiles – it looks more like a superhump modulation than an orbital modulation. The mean amplitude of the peaks is ~0.20 mag. From the discussion in the previous section, we would expect that any orbital modulation would appear at 70.0 ± 0.5 μHz, equivalent to a period of 3.94 ± 0.03 h. But there is no evidence for this in the FT. But not to despair – it was already pointed out in WW03 that the absence of a P_{orb} signal implies that V842 Cen probably has a low orbital inclination. On the other hand, the amplitudes of superhumps are known to be independent of inclination (e.g. Warner 1995), so the existence
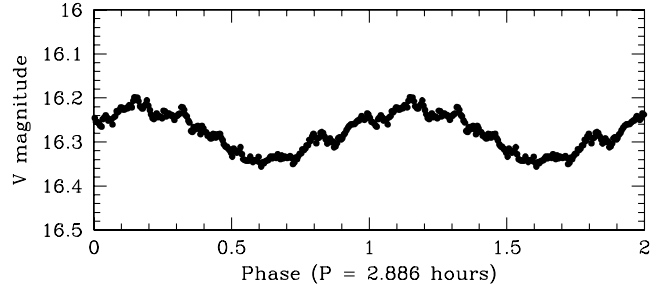

Figure 6. The low-frequency FT of the 2008 March observations. The 73.46-μHz frequency and its first three harmonics are marked by the vertical dashed lines.

Figure 7. The average light curve of V842 Cen (2008 March), folded on the 3.780-h superhump period.

Figure 8. A section of the light curve of run S7791. The ~350-s QPOs are marked by the vertical bars.

Figure 9. The average light curve of V842 Cen (2008 March), folded on the 2.886-h period.

of large amplitude superhumps is not a surprise. But what we see is that in V842 Cen they are negative superhumps, with a period 4.1 per cent shorter than the inferred P_{orb}. Again, we draw attention to the similarities between the light curve of V842 Cen and that of TT Ari, which has $P_{orb} = 3.30$ h and for much of the time negative superhumps at a period 3.4 per cent shorter (Skillman et al. 1998).

2.3 Quasi-periodic oscillations

We see no sign of any dwarf nova oscillations (DNOs), which might be expected with periods <60 s, but the light curves and FTs show occasional presence of QPOs over the range 350–1500 s, often with re-occurrence during a particular run. We show here only an example of a train of ~350 s QPOs in one of the light curves (Fig. 8).
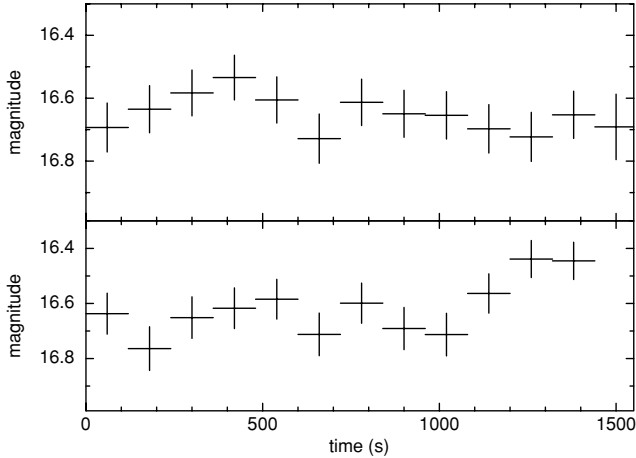
2.4 The 2.89-h modulation

The strong signal at 2.886 h is sinusoidal, as seen in the mean light curve of the 2008 March data (Fig. 9). This period bears no obvious relationship to the orbital or superhump periods; its ratio to P_{orb} is 1/1.37. Our only current suggestion is that it is another example of the mysterious 'GW Lib' phenomenon, of which other examples are given in table 2 of Woudt, Warner & Pretorius (2004). There, the periodic signals in GW Lib, Aqr1, FS Aur and HS 2331 are listed; the last named has a modulation with a period that is also smaller than its P_{orb}.

3 X-RAY AND UV OBSERVATIONS

The multi-wavelength *Swift* satellite (Gehrels et al. 2004) observed V842 Cen in 2008 July; the two twin-snapshot observations are summarized in Table 2. The target was clearly seen by the X-ray telescope in Photon Counting mode (Burrows et al. 2005) in both observations. The UV–optical telescope (Roming et al. 2005) was operated in the blocked filter wheel position for the first observation,

Table 2. *Swift* X-ray and UV observations.

2008 Date of obs. (UT)	XRT exp. (s)	XRT count rate (c/ks)	uvw1 (mag)
July 11 14:03–16:05	2998	7.4 ± 1.9	–
July 20 10:07–13:49	2954	7.9 ± 2.0	16.63 ± 0.02

Figure 10. *Swift* UVOT observations of V842 Cen taken in the uvw1 filter on 2008 July 20. The top panel starts at UT 10:06:55, the bottom panel at 13:24:55; the bin width is 120 s.

and with the uvw1 filter (central wavelength: 2600 angstroms) in event mode for the same exposure time as the X-ray telescope (XRT) in the second.

The data were reduced using version 2.9 of the *Swift* analysis software and calibration data base. XRT grade 0–12 0.3–10 keV events from V842 Cen were extracted from a 35 arcsec radius region around the source, with the background taken from a surrounding annulus; the count rates corrected for point spread function losses and bad pixels are given in Table 2. Like the count rates, XRT spectra from the two observations were compared and found to be consistent. We used XSPEC to perform unconstrained spectral fits to the total X-ray spectrum, fitting an optically thin plasma emission model (mekal) absorbed by cold gas (phabs); having just 35 source counts, we used Cash statistics in finding the best-fitting parameter values and their 90 per cent confidence errors. These are $N_H = (2.2^{+2.6}_{-1.7}) \times 10^{21}$ cm^{-2}, consistent with the reddening reported in Section 1, and $kT = 3.3^{+15.0}_{-1.5}$ keV; the best fit has C-stat = 34.5 for 32 bins. The observed 0.3–10 keV flux is 2.4×10^{-13} erg cm^{-2} s^{-1}, corresponding to a bolometric luminosity at 1 kpc of 5–8×10^{31} erg s^{-1}, where the range accounts for the uncertainty in the fitted parameters. We used standard Fourier and period-folding techniques, but with the small number of X-ray counts, it is not surprising that we find no evidence for variability at the periods reported in this work.

The UVOT uvw1 magnitudes were calculated by running the Ftool UVOTMAGHIST on the two sky images, using the standard source aperture of 5 arcsec. These magnitudes were consistent, and the flux-average magnitude is reported in Table 2. Cleaned UVOT event lists were created following the standard steps in the UVOT Users' Guide[1] and light curves extracted using UVOTEVTLC; they show mild variability (see Fig. 10) possibly like the quieter sections of the *V*-band light curves of Figs 1 and 2. We made fast FTs of the 1 s binned

UVOT light curves, but found no evidence of the 57-s period nor of the 350-s QPO; the two 1505-s and 1445-s light curves separated by 2.9 h do not allow a search for the longer periods. Folding the two light curves together at the 56.825-s period, we used sine wave fitting to derive a 90 per cent confidence upper limit to the modulation amplitude of <3 per cent. This can be compared to the 1150–2500 angstrom continuum DQ Her spin period amplitudes of 4.5 and <2 per cent measured by Silber et al. (1996).

4 DISCUSSION

A variety of brightness modulations have been found in other nova remnants. Of stable oscillations the best known, of course, is that at 71.1 s found in DQ Her (Nova Herculis 1934) by Walker (1956). A similar case was later found – the 63.63 s in V533 Her (Nova Herculis 1963), but was only visible for a few years (Patterson 1979). More recently, several other nova remnants have been found to have stable short periodicities (e.g. Nova Per 1901, 351 s: Watson, King & Osborne 1985; Nova Sct 1975, 258 s: Woudt & Warner 2003). From the essential mono-periodicity (though often with orbital sidebands) of these examples, and their similarity to the more slowly rotating IPs (see chapters 7 and 8 of Warner 1995), the periodicities in all such systems are ascribed to rotation of magnetic white dwarf primaries.

V842 Cen has the shortest white dwarf rotation period currently known for a nova remnant, and the third shortest known solid body rotation for any CV white dwarf – the other two being the nova-like AE Aqr ($P_{rot} = 33.06$ s) and the dwarf nova WZ Sge ($P_{rot} = 27.87$ s) (Warner & Pretorius 2008). There are reasons for classifying the shortest period IPs into a separate subclass – the DQ Herculis class (see introduction to chapter 8 of Warner 1995), in which case V842 Cen is the first far southern hemisphere DQ Her star.

DNOs, oscillations of lower coherence and short period, common among high $\dot{M}$ CVs such as dwarf novae in outburst and in nova-like variables, and DNO-related QPOs (for a review, see Warner 2004), have been found in only two nova remnants, namely RR Pic (Nova Pictoris 1925), where transient oscillations are seen in the range 20–40 s, with preference for ∼32 s (Schoembs & Stoltz 1981; Warner 1981) and GK Per, where ∼5000 s oscillations are related to the 351 s rotation of the primary (Hellier, Harmer & Beardmore 2004). A current explanation for DNOs is found in magnetic accretion from the inner regions of the accretion disc on to a low inertia, slipping equatorial accretion belt. If the primary has a field strong enough to prevent the formation of a slipping equatorial belt DNOs are not expected, leading to mutual exclusion of DNOs and solid body rotational signals (Warner 2004), which is as seen in V842 Cen.

General kilosecond QPOs, although common in nova-likes, are also found in only a few novae (e.g. BT Mon and V533 Her; Warner 2004). But here again there is similarity between V842 Cen and TT Ari – the latter has QPOs extending over the range 900–1500 s (Kim et al. 2009).

The lack of observable modulation in the *Swift* data from V842 Cen is not constraining. However, the bolometric X-ray luminosity of 5–8×10^{31} erg s^{-1} is significantly lower than the values for the IPs tabulated by Warner (1995) and the average quiescent $< L_{Bol} > \sim 3 \times 10^{33}$ erg s^{-1} derivable from Ezuka & Ishida (1999) when distance is accounted for. We note that DQ Her has a 0.5–2 keV luminosity of 3×10^{30} erg s^{-1} (Mukai et al. 2003), but in this case the high system inclination is believed to block a direct view of the accretion regions. Because many IPs have complex X-ray absorption, and we do not have many counts in the X-ray

[1] http://swift.gsfc.nasa.gov/docs/swift/analysis/

spectrum of V842 Cen, it is possible that our simple spectral model underestimates its true luminosity (and maximum temperature). Even so, a relatively low accretion rate for this IP would appear to be a natural conclusion.

The spectroscopic evidence that V842 Cen could have a low $\dot{M}$ (Section 1, above) is in conflict with the photometric results: a precessing disc, as deduced from the presence of superhumps, is a characteristic of a high $\dot{M}$ system, especially if the orbital period is greater than 3 h (e.g. Murray, Warner & Wickramasinghe 2000). However, a lessening $\dot{M}$, resulting from reduction of irradiation-driven mass loss as the white dwarf cools after eruption, would be expected, and this could be the reason for the appearance of the rotation modulation between 2002 and 2008. Indeed, the almost universal absence of DNOs among nova remnants is probably caused by the post-eruption high $\dot{M}$ crushing weak magnetospheres down to the surface of the primary. Only strong fields can make their presence known in the decades after eruption – these are the four nova remnants that are certain IPs, with another 13 possibles (Mukai 2008).

REFERENCES

Andrea J., Drechsel H., Starrfield S., 1994, A&A, 291, 869
Burrows D. N. et al., 2005, Space Sci. Rev., 120, 165
Downes R. A., Duerbeck H. W., 2000, AJ, 120, 2007
Duerbeck H. W., 1981, PASP, 93, 165
Ezuka H., Ishida M., 1999, ApJS, 120, 277
Gehrels N. et al., 2004, ApJ, 611, 1005
Gill C. D., O'Brien T. J., 1998, MNRAS, 300, 221
González-Riestra R., Orio M., Gallagher J., 1998, A&AS, 129, 23
Hellier C., Harmer S., Beardmore A. P., 2004, MNRAS, 349, 710
Horne K., Welsh W. F., Wade R. A., 1993, ApJ, 410, 357
Iben I., Jr, 1992, in Warner B., ed., ASP Conf. Ser. Vol. 30, Variable Stars and Galaxies. Astron. Soc. Pac., San Francisco, p. 307
Kim Y., Andronov I. L., Cha S. M., Chinarova L. L., Yoon J.-N., 2009, A&A, in press
McNaught R. H., 1986, IAU Circ., 4274, 1
Mukai K., Still M., Ringwald F. A., 2003, ApJ, 594, 428
Mukai K., 2008, http://asd.gsfc.nasa.gov/Koji.Mukai/iphome/catalog/alpha.html
Murray J. R., Warner B., Wickramasinghe D. T., 2000, MNRAS, 315, 707
O'Donoghue D., 1995, Balt. Astron., 4, 517
Patterson J., 1979, ApJ, 233, L13
Robinson E. L., 1975, AJ, 80, 515
Roming P. W. A. et al., 2005, Space Sci. Rev., 120, 95
Schmidtobreick L., Tappert C., Bianchini A., Mennickent R. E., 2005, A&A, 432, 199
Schoembs R., Stoltz B., 1981, Inf. Bull. Variable Stars, 1986, 1
Sekiguchi K., Feast M. W., Fairall A. P., Winkler H., 1989, MNRAS, 241, 311
Silber A. D., Anderson S. F., Margon B., Downes R. A., 1996, ApJ, 462, 428
Skillman D. T. et al., 1998, ApJ, 503, L67
Walker M. F., 1956, ApJ, 123, 68
Warner B., 1981, MNRAS, 195, 101
Warner B., 1986, MNRAS, 219, 347
Warner B., 1995, Cataclysmic Variable Stars. Cambridge Univ. Press, Cambridge
Warner B., 2002, in Hernanz M., José J., eds, AIP Conf. Proc. Vol. 637, Classical Nova Explosions. Am. Inst. Phys., New York, p. 3
Warner B., 2004, PASP, 116, 115
Warner B., Pretorius M. L., 2008, MNRAS, 383, 1469
Watson M. G., King A. R., Osborne J., 1985, MNRAS, 212, 917
Woudt P. A., Warner B., 2003, MNRAS, 340, 1011 (WW03)
Woudt P. A., Warner B., Pretorius M. L., 2004, MNRAS, 351, 1015

This paper has been typeset from a TEX/LATEX file prepared by the author.